Reactivity of Ebtellur Derivatives with the Peroxynitrite Anion: Comparison with Their Ebselen Analogues

Yukiko Sakimoto and Kimihiko Hirao*

Department of Applied Chemistry, School of Engineering, The University of Tokyo, Tokyo 113-8656, Japan

Djamaladdin G. Musaev*

Cherry L. Emerson Center for Scientific Computation, Emory University, Atlanta, Georgia 30322

Received: May 2, 2003; In Final Form: May 19, 2003

The mechanism of the reaction of an ebtellur derivative **2__Te**, [1,2-benzisotellurazol-3(2*H*)-one], with peroxynitrite anion, $ONOO^-$ (PN), was studied at the density functional (B3LYP) level using triple-ζ quality basis sets. It was shown that the reaction proceeds via the pathway **2__Te** + PN → **2__Te−PN** → **2__Te-TS1 (O−O activ)** → **2__Te−O(NO_2^-)**. From the intermediate **2__Te−O(NO_2^-)** it splits into two distinct pathways, NO_2^- dissociation leading to **2__Te−O** + **NO_2^-** and NO_3^- formation via the transition state **2__Te-TS2**. These two pathways proceed with $\Delta H = 36.6$ ($\Delta G = 25.9$) and 26.6 (26.9) kcal/mol energy loss, respectively. The inclusion of the strongest electron-withdrawing substituent, R = CF_3, creating complex **4__Te**, effectively pushes the reaction toward the peroxynitrite → nitrate isomerization in the gas phase. The comparison of these data with our previous results (Musaev, D. G.; Geletii, Y. A.; Hill, G.; Hirao, K. *J. Am. Chem. Soc.* **2003**, *125*, 3877) on the reaction of ebselen derivatives with PN indicates that the probability of peroxynitrite → nitrate isomerization is higher for ebtellur than ebselen derivatives in the gas phase. It is predicted that the ebselen and ebtellur derivatives with nonexistent (or weak) M−N^2 bonds will be more active in the steps of PN coordination, O−O bond cleavage, and nitrate formation. Meanwhile, the ebselen and ebtellur derivatives with strong M−N^2 bonds are predicted to be useful for NO_2^- dissociation and selenoxide formation. The inclusion of solvent effects at the polarizable continuum model (PCM) level makes the reaction **2__Te** + PN more facile and stabilizes the NO_2^- dissociation pathway over the nitrate formation one. It makes the peroxynitrite ↔ nitrate isomerization practically impossible.

I. Introduction

Peroxynitrite anion ($ONOO^-$, PN) has attracted great interest over the past several decades.[1] (The term peroxynitrite is used to refer to the peroxynitrite anion $O{=}NOO^-$, and peroxynitrous acid, HOONO, unless otherwise indicated. The IUPAC recommended names are oxoperoxonitrate (−1) and hydrogen oxoperoxonitrate, respectively. In this paper, the abbreviation PN is used to refer to the peroxynitrite anion $O{=}NOO^-$.) It is fairly stable in alkaline solution,[2] but quickly isomerizes to nitrate upon protonation ($pK_a = 6.8$).[2−4] On its way to nitrate, peroxynitrous acid HOONO may produce highly reactive •OH and NO_2• radicals (or an •OH···NO_2• "cage-radical").[2b,5] Both PN and HOONO, as well as the radicals •OH and NO_2• react rapidly with numerous biomolecules, including proteins, lipids, DNA, antioxidants, and aromatic compounds.[6−14] The high reactivity of peroxynitrite (and related radicals) with various biological targets implicates it in many disease states.[15] Therefore, the search for drugs that can intercept this powerful oxidizing and nitrating agent and detoxify it becomes one of the major tasks of pharmaceutical and chemical sciences.

One of the effective exogenous defense lines against PN toxicity is glutathione peroxidase (GPx), a selenium-containing enzyme that destroys peroxides through their catalytic reduction by thiol glutathione (GSH).[16] Therefore, in the search for drugs against peroxynitrite, a variety of organic selenium compounds that mimic the GPx enzyme have been proposed.[17] Among these species, ebselen (Chart 1), which has been identified as an anti-inflammatory agent,[18] is one of the most promising. Although it reacts[19] with PN with a rate constant of 2.0×10^6 M^{-1} s^{-1},[20] it shows poor GPx activity. Therefore, the search for better selenium-containing antioxidants is continuing. For example, recently,[21] it was reported that allyl 3-hydroxypropyl selenide exhibits better GPx activity than ebselen.

CHART 1: Schematic Presentation of the Se- and Te-Compounds Used in This Paper

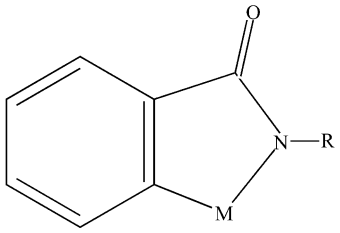

M= Se and R=Ph	-	**1**, **Ebselen**
M= Se and R=H	-	**2_Se**
M= Se and R=CF_3	-	**4_Se**
M= Te and R=Ph	-	**1**, **Ebtellur**
M= Te and R=H	-	**2_Te**
M= Te and R=CF_3	-	**4_Te**

Simultaneously, the focus of experimental studies has extended to the organotellurium analogues of the organoselenium compounds. It has been demonstrated that some organotellurium compounds exhibit potent antioxidative properties and higher GPx-like activity than their selenium analogues.[22−25] Furthermore, different peroxynitrite reduction rates for organoselenium

10.1021/jp035191h CCC: $25.00
Published on Web 06/25/2003

and analogous organotellurium compounds were reported. This was interpreted in terms of both a basic difference between the reaction mechanisms of selenides and tellurides and their having different rate-determining steps.[23] We believe that the elucidation of the differences and similarities of the organoselenium and analogous organotellurium compounds could be extremely important for designing better antioxidants against peroxynitrite.

Therefore, the goals of this paper are (a) to elucidate the mechanisms and the factors affecting the mechanisms of the reaction of ebtellur (tellurium analogue of ebselen) with peroxynitrite and (b) to compare the results for ebtellur with those for the analogous reaction of ebselen, reported earlier.[26,27]

We have previously studied the mechanism of the reaction of ebselen (**1**) and its derivatives (**2**−**7**) (Scheme 1) with $ONOO^-$[26] and HOONO.[27] It was demonstrated that the reaction of complex **2** (the model of ebselen, which will be denoted as **2__Se** in this paper) with PN proceeds via the pathway: **2__Se** + PN → **2__Se**−**PN** → **2__Se-TS1 (O**−**O activ)** → **2__Se-(O)-(NO_2^-)** → **2__Se**−**O** + NO_2^-. In general, from the complex **2__Se**−**(O)(NO_2^-)**, the reaction may split into the second possible pathway of NO_3^- formation. However, this pathway was shown to be less favorable for ebselen in solution.

In this paper, we elaborate the same mechanism of the reaction of **2__Te** with PN. We compare the results for **2__Se**, studied previously, and **2__Te**, reported in this paper. These studies will allow us to elucidate similarities and differences in the reactivities of ebselen and ebtellur, which could be crucial in designing better antioxidants against peroxynitrite.

II. Calculation Procedures

All calculations were performed with the quantum chemical package GAUSSIAN-98.[28] The geometries, vibrational frequencies, and energetics of all structures were calculated using the hybrid density functional theory, B3LYP.[29] In these calculations we used the 6-311+G(d,p) split-valence basis sets for all atoms except Te. For Te, we used the Stuttgart−Dresden relativistic effective core potential and associated basis set.[30] The combination of these basis sets will be called BS1.

To test the accuracy of the B3LYP/BS1 approach used in this paper, we calculated the geometries of the molecules Te_2, TeO, and TeH_2 and compared our findings with the available experimental data.[31] This comparison shows that the B3LYP/BS1 approach provides very good agreement with the experiment. Indeed, the B3LYP/BS1 calculated bond distances in Te_2, TeO, and TeH_2 are 2.657, 1.860, and 1.652 Å, compared to their experimental values of 2.556, 1.825, and 1.658 Å, respectively. Similarly, the calculated bond angle in TeH_2, 90.8°, is very close to its experimental value of 89.5°.

Previous studies[32] on the structure and stabilities of *cis*- and *trans*-$ONOO^-$ as well as their protonated forms show that the B3LYP and the more sophisticated CCSD(T), G2, and CBS-Q approaches using the 6-311+G(d,p) basis sets provide very close agreement. Meanwhile, we[27] and others[33] have demonstrated that the B3LYP/6-311+G(d,p) approach underestimates the calculated energetic barriers by about 5 kcal/mol compared to the CCSD(T) and QCISD(T) methods. In the current paper, we discuss relative energies calculated at the same level of theory; therefore, we believe that any underestimation of the calculated barriers by the B3LYP method will not affect our general conclusions. Note that the same approaches were used in our previous studies on ebselen.[27]

III. Results and Discussion

This paper is organized as follows. First, in section III.1, we discuss the mechanism of the reaction **2__Te** + PN in the gas phase. We compare the potential energy surfaces (PESs) of the reactions of **2__Te** and **2__Se** with PN in section III.2. In section III.3, we discuss the roles of the solvent effects, while in the final section, section IV, we draw some conclusions from our studies.

Note that the peroxynitrite anion $ONOO^-$, as well as the possible nitrogen-containing products of the reaction of **2__Te** with $ONOO^-$, the molecules NO_2, NO_2^-, and NO_3^-, have been the subject of numerous studies.[34] Therefore, here we will discuss those molecules only very briefly, as necessary, while we include their calculated geometries and energetics in Tables 1S and 2S of the Supporting Information.

III.1. Mechanism of the Reaction of 2__Te with $ONOO^-$ in the Gas Phase. In general, it was found that PN has two different isomers, cis and trans, among which the cis isomer is reported to be 2-4 kcal/mol more stable than the trans isomer.[32,35] These isomers are separated by a 21−27 kcal/mol barrier, corresponding to rotation around the ON−OO bond.

The calculated important geometrical parameters of the complex **2__Te** are given in Figure 1. As shown there, the complex **2__Te,** which is the simplest ebtellur derivative, is a planar molecule with strong $Te-C^1$ and $Te-N^2$ bonds of 2.114 and 2.058 Å, respectively.

The first intermediate of the reaction **2__Te** + **PN** is expected to be the molecular complex **2__Te**−**PN**. As expected, this complex forms by coordination of the negatively charged O^3 end of PN to the positively charged Te center of **2__Te**. Since PN has two different isomers, cis and trans, each of them could coordinate to Te center of **2__Te** via two different orientations, cis and trans, relative to the $Te-N^2$ bond, and form various isomers, such as cis-cis, cis-trans, trans-cis, and trans-trans. Here, the first definition stands for the isomer of PN and the second definition stands for the position where PN coordinates (Figure 1). Furthermore, each of these isomers may have several additional forms, which could be classified by the rotation of the $O^1N^1O^2$ unit around the O^2-O^3 bond.

We first studied the coordination of the most favorable cis isomer of PN via cis and trans to the $Te-N^2$ bond. We have identified three different isomers of the **2__Te**−**PN** complex corresponding to the different coordination modes of *cis*-PN and **2__Te**, namely *cis-cis_1*, *cis-cis_2,* and *cis-trans* (Figure 1). As seen in Table 1, among these three isomers the *cis-trans* is energetically the most stable and lies $\Delta H = 39.9$ ($\Delta G = 28.9$) kcal/mol lower than the reactants. The *cis-cis_1* and *cis-cis_2* isomers, which are almost equivalent (the energy difference between them is only 0.2−0.3 kcal/mol), are about 9 kcal/mol higher than *cis-trans*. The lower stability of the *cis-cis* isomers compared to the *cis-trans* could be explained by the existence of a strong trans effect from the $Te-C^1$ bond in the *cis-cis* isomers compared to the $Te-N^2$ effect in the *cis-trans* isomer. Note that another possible *cis-trans* isomer, with the $O^1N^1O^2$ unit located on the Ph-ring side, is energetically unfavorable and converges to **2__Te**−**PN-*cis-trans***.

Thus, these results show that the cis coordination of *cis*-PN to **2__Te** is energetically less favorable than its trans coordination. Therefore, for *trans*-PN we have studied only the trans coordination, leading to two different isomers **2__Te**−**PN-*trans-trans*__1** and **2__Te**−**PN-*trans-trans*__2**. (The geometries of these isomers are presented in the Supporting Information; see Table 1S and Figure 1S). As seen in Table 1, they are again degenerate with an energy difference of about 0.5−0.8 kcal/mol.

Thus, coordination of *cis*- and *trans*-PN to complex **2__Te** leads to the formation of numerous isomers, which can easily

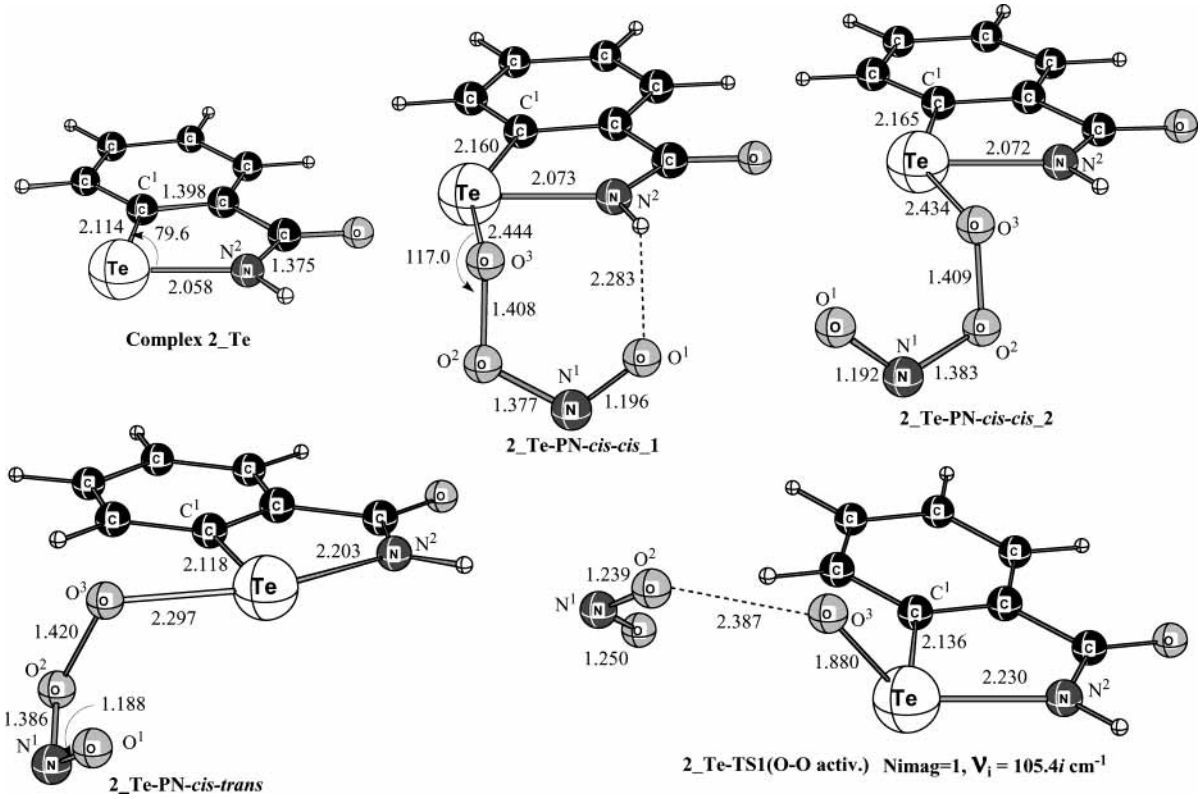

Figure 1. Calculated important geometries (distances in Å, angles in deg) of the reactant, **2__Te**, various isomers of the **2__Te-PN** complex, and the O−O activation transition state **2__Te-TS1**. The full geometries parameters of these species are given in Table 1S of the Supporting Information.

TABLE 1: B3LYP/BS1 Relative Energetics (in kcal/mol) of the Intermediates, Transition States, and Products of the Reactions of 2__Te (Relative to the Reactants) and 4__Te (Relative to the Intermediate 4__Te−O(NO$_2$)__1) with OONO$^-$ (PN)′

	gas phase				water
structures	ΔE_{tot}	ΔE_{tot} + ZPC	ΔH	ΔG	ΔG(sol)[a]
R = H					
2__Te + *cis*-OONO$^-$	0.0	0.0	0.0	0.0	0.0
2__Te−PN-cis-cis__1	−31.9	−30.8	−30.6	−19.3	
2__Te−PN-cis-cis__2	−31.7	−30.7	−30.4	−19.7	
2__Te−PN-cis-trans	−41.3	−40.1	−39.9	−28.6	−11.0
2__Te−PN-trans-trans__1	−38.2	−37.2	−36.9	−25.6	
2__Te−PN-trans-trans__2	−38.7	−37.7	−37.4	−26.4	
TS1(O−O activ.)	−29.5	−29.6	−29.2	−18.8	−6.8
TS1(O−O activ.)__2	−19.7	−19.4	−19.4	−7.6	
2__Te−O(NO$_2$)__1	−64.1	−63.3	−62.8	−51.9	−42.4
2__Te−O(NO$_2$)__2	−63.5	−62.6	−62.1	−51.6	
2__Te−O(NO$_2$)__3	−60.2	−58.9	−58.5	−47.6	
2__Te−NO$_3^-$	−82.0	−79.3	−79.3	−68.1	−52.4
2__Te−TS2(O−NO$_2$ form.)	−36.8	−36.4	−36.2	−25.0	−13.1
2__Te + NO$_3^-$	−54.1	−52.4	−52.7	−52.2	−51.4
2__Te−O + NO$_2^-$	−26.3	−26.5	−26.2	−26.0	−33.4
R = CF$_3$					
4__Te −O(NO$_2$)__1	0.0	0.0	0.0	0.0	0.0
4__Te−O + NO$_2^-$	47.7	46.8	46.6	35.7	15.4
4__Te−TS2(O−NO$_2$ form.)	23.3	23.0	22.7	23.0	26.4

[a] This should be compared with ΔE_{tot} of the gas phase (see text for more details).

rearrange to each other with very small rotational barriers (which were not calculated because their role in the overall reaction mechanism was thought to be negligible). Because among these isomers the **2__Te−PN-*cis-trans*** is energetically the lowest, we will discuss the processes starting from this isomer.

As seen in Figure 1, the coordination of *cis*-PN and *trans*-PN via the trans position to Te−N^2 of **2__Te** elongates the Te−N^2 bond by 0.14−0.15 Å, compared with that in the free **2__Te**. As expected, the coordination of PN to complex **2__Te** also changes the geometry of the ONOO$^-$ unit. However, these changes are insignificant and will not be discussed in detail.

In the next stage of the reaction, the O^3−O^2 bond cleavage occurs via the transition state **2__Te-TS1** (Figure 1), which was positively characterized and has only one imaginary frequency (105.4*i* cm^{-1}) corresponding to the O^3−O^2 cleavage. Intrinsic reaction coordinate (IRC)[36] calculations show that this transition state connects the complex **2__Te−PN-*cis*−*trans*** and product **2__Te−O(ONO)**. As shown in Figure 1, in **2__Te-TS1** the O^3−O^2 bond length is elongated by 0.967 Å, while the Te−O^3 and N^1−O^2 bond lengths are shortened by 0.417 and 0.147 Å, respectively, compared with those in the pre-reaction complex **2__Te−PN-*cis-trans***. All these geometrical changes are consistent with the nature of this transition state, where the O^3−O^2 bond cleavage and the Te−O^3 and N^1═O^2 double bond formation occurs. The Te−C^1 and Te−N^2 bonds located trans to the formed Te−O^3 bond are also slightly (0.02−0.03 Å) elongated because during this process the strong Te−O^3 bond forms.

Transition state **2__Te-TS1** is found to be 29.2 (18.8) kcal/mol lower than reactants. Meanwhile, the calculated O^3−O^2 bond cleavage barrier from the pre-reaction complex **2__Te−PN-*cis-trans*** is 10.7 (10.1) kcal/mol.

Note that we are aware of the existence of several different O^3−O^2 activation transition states connecting different isomers of **2__Te−PN** (discussed above) with those of **2__Te−O(ONO)** (see below). For example, we have located the transition state **2__Te-TS1__cis** (see Table 1S and Figure 1S in the Supporting Information) corresponding to the O^3−O^2 bond cleavage in the complex **2__Te−PN-*cis-cis*__1**. However, it lies significantly higher in energy than **2__Te-TS1** (see Table 1) and will not be discussed. Furthermore, we do not expect that the other possible

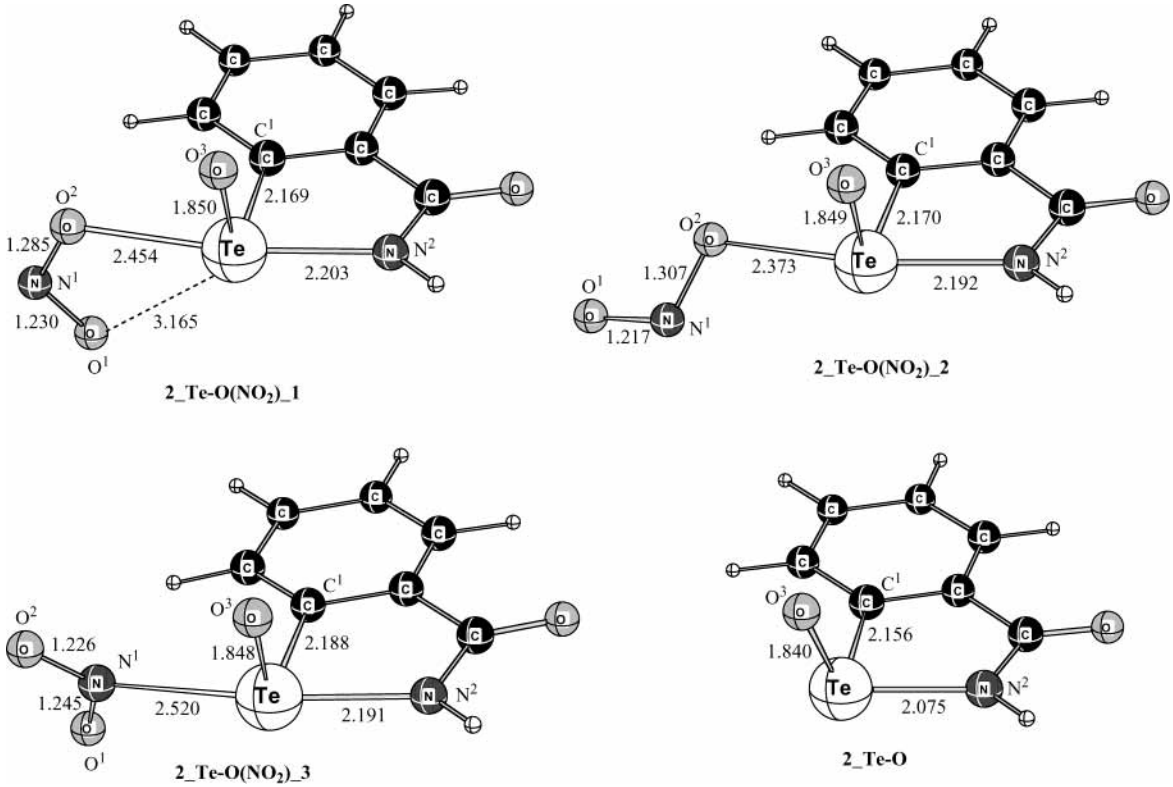

Figure 2. Calculated important geometrical parameters (distances in Å, angles in deg) of the O−O activation products, various isomers of the **2__Te-O(NO$_2$)** complex, and the complex **2__Te-O**. The full geometries parameters of these species are given in Table 1S of the Supporting Information.

O−O cleavage transition states will be significantly different from **2__Te-TS1** and **2__Te-TS1__cis** and, therefore, can be ignored.

It is noteworthy that the O^3-O^2 bond cleavage by the compound **2__Te** can be considered a heterolytic process similar to O-atom transfer, which is common in organometallic chemistry.[37]

The product of the O−O bond cleavage is the complex **2__Te−O(NO$_2$)**, as shown by IRC calculations performed from the **2__Te-TS1**. However, the resulting complex may have various isomers, three of which are presented in Figure 2. Among these three isomers, **2__Te−O(NO$_2$)__1** and **2__Te−O(NO$_2$)__2** are almost energetically degenerate, while the isomer **2__Te−O(NO$_2$)__3** lies only 4.3 (4.3) kcal/mol higher than isomer **2__Te−O(NO$_2$)__1** (see Table 1). As shown previously[26] for ebselen, **2__Se**, the complex **2-O(NO$_2$)** may have even more isomers. However, we expect all these isomers to be close to each other in energy and separated by only small energetic barriers. Therefore, we did not identify all possible isomers and transition states for complex **2__Te−O(NO$_2$)**. We believe that these will not affect our conclusions. Below, for simplicity, we discuss geometries of the most stable isomer **2__Te−O (NO$_2$)__1**, which is a product of the O−O bond activation via the transition state **2__Te-TS1**, and the important processes starting from this isomer.

As seen in Figure 2, in **2__Te−O(NO$_2$)__1**, the Te=O^3 double bond, with a bond length of 1.850 Å, is located out of the Te-(C_6H_4CONH) plane. Furthermore, the NO_2 unit is bound to the Te-center trans to the Te−N^2 (the weakest) bond. Interestingly, despite the formation of the strong Te=O^3 bond, the Te−N^2 bond in **2__Te−O(NO$_2$)__1** is slightly (0.027 Å) shorter than that in the corresponding O^2-O^3 activation transition state **2__Te-TS1**. In other words, after O^2-O^3 bond cleavage, the Te−N^2 bond partially recovers.

The product **2__Te−O(NO$_2$)** is a complex of NO_2^- anion and OTe(C_6H_4CONH) molecule. Its lowest isomer, **2__Te−O(NO$_2$)__1**, lies 62.8 (51.9) kcal/mol lower than the reactants and 22.9 (23.0) kcal/mol lower than the corresponding **2__Te−PN-*cis-trans*** complex (see Table 1).

From the complex **2__Te−O(NO$_2$)** the reaction may split into two distinct channels, NO_2^- dissociation and telluroxide formation, and/or nitrate (NO_3^-) formation (peroxynitrite → nitrate isomerization). Let us discuss these processes separately.

Our calculations show that the NO_2^- dissociation from the complex **2__Te−O(NO$_2$)__1** to give **2__TeO** occurs without a barrier and is endothermic by 36.6 (25.9) kcal/mol. The final products, **2__TeO** + **NO_2^-**, lie 26.2 (26.0) kcal/mol lower than the reactants **2__Te** + PN. As seen in Figure 2, dissociation of NO_2^- results in complete recovery of the Te−N^2 bond: the calculated Te−N^2 bond length is 2.075 Å in **2__TeO**, which is close to the value of 2.058 Å found in the reactant **2__Te**.

The second process starting from the **2__Te−O(NO$_2$)__1** complex is NO_3^- formation, which occurs via the transition state **2__Te-TS2**, shown in Figure 3. Normal-mode analysis shows that this is a real transition state with one imaginary frequency of 200.4*i* cm^{-1} corresponding to the formation of the N^1-O^3 bond. The N^1-O^3 bond length in **2__Te-TS2** is calculated to be 2.347 Å, which is significantly smaller than that in the pre-reaction complex **2__Te−O(NO$_2$)__1** of 4.270 Å. Meanwhile, the Te−O^3 bond length in **2__Te-TS2** is elongated by 0.033 Å compared with that in the pre-reaction complex **2__Te−O(NO$_2$)__1**. These data show that the transition state **2__Te-TS2** is a relatively early transition state: its important geometrical parameters are close to those in the pre-reaction complex. IRC calculations show that **2__Te-TS2** connects the complex **2__Te−O(NO$_2$)__2** with the product **2__Te−NO_3^-** shown in Figure 3.

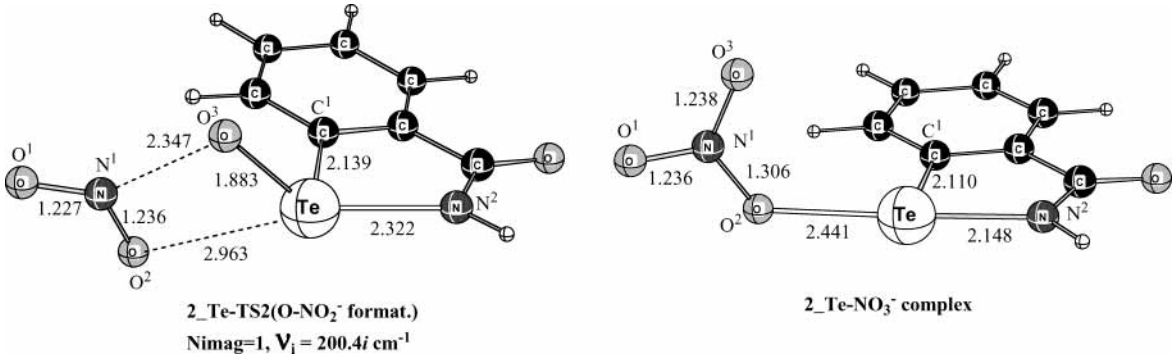

Figure 3. Calculated important geometrical parameters (distances in Å, angles in deg) of the NO^3 formation transition state, **2__Te-TS2(O-(NO_2 format)** and **2__Te-NO_3^-** complex.

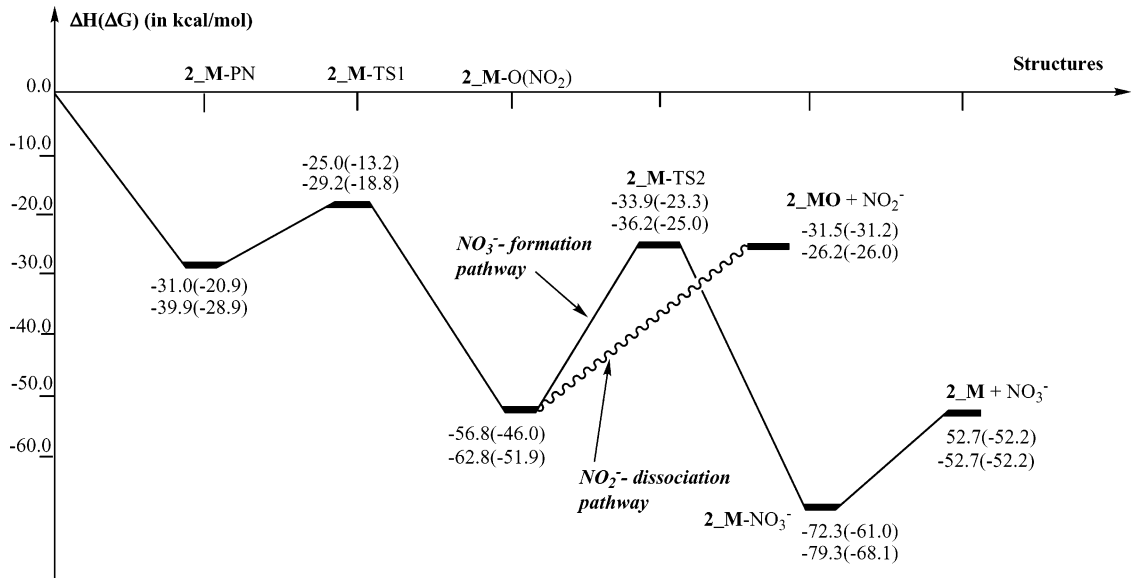

Figure 4. Schematic representation (based on Δ*G* values) of potential energy surfaces of the reaction **2__M** + PN, for M = Se the first line) and M = Te (the second line) calculated at the B3LYP/6-311+G(d,p) and B3LYP/BS1 levels, respectively. Here, we have presented energies of only the lowest possible isomers of calculated intermediates and transition states. The numbers outside the parentheses are Δ*H* values, while those inside the parentheses are Δ*G* values.

The barrier height at the transition state **2__Te-TS2** is 26.6 (26.9) kcal/mol calculated from the complex **2__Te−O(NO_2)__1** (which is energetically almost degenerate with **2__Te−O-(NO_2)__2**).

In the resulting complex **2__Te−NO_3^-**, the NO_3^- ligand is already formed and coordinated to the Te-center of **2__Te** through one of its O^2-atoms (Figure 3). The calculated Te−O^2 bond length is 2.441 Å. Meanwhile, the calculated Te−N^2 bond length in **2__Te−NO_3^-**, 2.148 Å, is slightly shorter than that in **2__Te−O(NO_2)__1**, 2.203 Å, indicating that NO_3^- is a weaker trans ligand than NO_2^-. Indeed, the calculations show that the Te−NO_3^- binding energy in **2__Te−NO_3^-** is 26.6 (15.9) kcal/mol vs 36.6 (25.9) kcal/mol Te−NO_2^- binding energy in **2__Te−O(NO_2)__1**. Complex **2__Te−NO_3^-** is calculated to be about 16.5 (16.2) kcal/mol more stable than the pre-reaction complex **2__Te−O(NO_2)__1**. The entire process, **2__Te** + PN → **2__Te** + NO_3^-, is found to be exothermic by 52.7 (52.2) kcal/mol.

III.2. Comparison of the Potential Energy Surfaces (PESs) of the Reaction 2__M + PN for M = Se and Te. The overall PESs of the reaction **2__M** + PN for M = Se and Te are presented in Figure 4.

As Figure 4 shows, the coordination of PN to **2__M** is about 8.9 (8.0) kcal/mol more exothermic for M = Te than for M = Se, which is consistent with the fact that organo-tellurium compounds are more nucleophilic than their selenium analogues.[38] However, the calculated O^2-O^3 cleavage barrier is larger for ebtellur than ebselen: for ebtellur it is found to be 10.7 (10.1) kcal/mol, while for ebselen it is 6.0 (7.7) kcal/mol. The product of the O^2-O^3 cleavage, **2__M−O(NO_2)**, is an **(NO_2^-)-2__MO** type of complex and is again more stable for M = Te than for M = Se: it lies 62.8 (51.9) and 56.8 (46.0) kcal/mol lower than the reactants for M = Te and Se, respectively. This trend is not correlated with the fact that the Te=O bond (92.5 ± 2 kcal/mol) is smaller than the Se=O bond (100 ± 3 kcal/mol),[31] and indicates that NO_2^- binds more strongly to **2__Te=O** than to **2__Se=O**. Indeed, our calculations show that the NO_2^- dissociation energy from **2__M−O(NO_2)** is larger for M = Te than for M = Se: 36.6 (25.9) vs 25.3 (14.8) kcal/mol.

The second process, nitrate formation, starting from the same **2__M−O(NO_2)** complex, also occurs with a slightly larger barrier for M = Te than for M = Se: it occurs with 26.6 (26.9) and 22.9 (22.7) kcal/mol barriers at the transition state **2__M-TS2** for M = Te and Se, respectively. The resulting **2__M-NO_3^-** complex again lies slightly lower by energy than the reactants for M = Te than for M = Se and is more stable relative to the dissociation limit of **2__M** + **NO_3^-**.

Thus, in the gas phase, the processes of NO_2^- dissociation and NO_3^- formation starting from the complex **2__M−O(NO_2)**

are rate-determining steps of the entire **2__M** + **PN** reaction for both Te and Se. However, for M = Se the barrier for nitrate formation is ΔG = (22.7) kcal/mol, while the NO_2^- dissociation requires significantly, (7.9) kcal/mol, less energy. Therefore, for M = Se the nitrate formation process is unlikely to compete with the NO_2^- dissociation, and *the products of the reaction* ***2__Se*** + ***PN*** *will be* NO_2^- *and selenoxide in the gas phase. Thus, in the gas phase the peroxynitrite → nitrate isomerization catalyzed by complex* ***2__Se*** *is highly unlikely.*[39] Meanwhile, for M = Te the nitrate formation barrier, ΔG = (26.9) kcal/mol, is only 1.0 kcal/mol higher than the NO_2^- dissociation energy, (25.9) kcal/mol, *which indicates that the formation of nitrate will compete with* NO_2^- *dissociation during the reaction of ebtellur with PN in the gas phase.* In other words, *the probability of peroxynitrite to nitrate isomerization is higher for ebtellur than ebselen in the gas phase.*

Furthermore, the analysis of the important geometrical parameters along the PES of the reaction **2__M** + **PN** shows that the M−N^2 bond is very flexible and changes significantly during the reaction, thus facilitating it. In the first step of the reaction, coordination of PN to **2__M**, the Te−N^2 bond elongates. In the next step, the O^3−O^2 cleavage, it elongates further to facilitate the M−O^3 bond formation, and consequently, the O^3−O^2 bond cleavage. The re-organization of geometrical parameters, especially movement of the M−O^3 bond from trans to cis with respect to the M−N^2 bond, most likely occurs in the close vicinity of the O^3−O^2 cleavage transition state and results in the partial recovery of the M−N^2 bond. After dissociation of NO_2^-, the M−N^2 bond almost fully recovers and reduces the endothermicity of this step of the reaction. On the basis of these observations we predict that ebtellur and ebselen derivatives similar to **2__M**, but with no M−N^2 bond, will be extremely active in the first part of the reaction, i.e., for the PN coordination and O−O bond cleavage. At the same time, ebtellur and ebselen derivatives such as compound **2__M**, but with a strong M−N^2 bond, will be extremely desirable for the NO_2^- dissociation.

In addition, the M−N^2 bond length significantly elongates at the transition state **2__M-TS2** compared with the pre-reaction complex **2__M−O(NO_2)__1** and facilitates the reaction. Therefore, we expect that catalysts similar to complex **2**, but with a weak or nonexistent M−N^2 bond, will facilitate the NO_3^- formation process. However, having a weak or nonexistent M−N^2 bond in the reactant complex may hamper the final step, NO_3^- dissociation, which is expected to be easier for complexes with strong M−N^2 bonds.

In summary, *we may expect that ebselen and ebtellur derivatives with nonexistent (or extremely weak)* M−N^2 *bonds (or any M−X bond, where X is bound to the* N^2*-center) may facilitate the peroxynitrite → nitrate isomerization process.*

To test these ideas and elucidate the roles of electronic effects (the role of Se−N^2 bond strength) in the NO_2^- dissociation and NO_3^- formation steps of the reaction of ebselen derivatives with PN, in our previous paper[26] we replaced the H ligand bound to the N^2 by the electron-withdrawing CH_3, C_6H_5, and CF_3 groups. We demonstrated that the energy difference, Δ, between the rate-determining steps of NO_2^- dissociation and NO_3^- formation, increases with the increasing electron-withdrawing ability of the group R in the order of H (2.6) ≈ CH_3 (2.0) < C_6H_5 (8.1) < CF_3 (14.8). On the basis of these studies, we predicted that the ebselen derivative with the strongest electron-withdrawing group R = CF_3 could be a good catalyst for peroxynitrite → nitrite isomerization in the gas phase. For the reaction of **2__Te** with $ONOO^-$, the energy difference, Δ, between the rate-determining steps of NO_2^- dissociation and NO_3^- formation is very small, −10.0 (1.0) kcal/mol (here "−" indicates that the **TS2** is energetically lower than the **2__TeO** + NO_2^- dissociation limit), so we may expect that the replacement of the H ligand bound to the N^2 by a CF_3 group in ebtellur derivatives will significantly enhance the peroxynitrite → nitrate isomerization. To test this expectation we investigated the important intermediates and transition states of the reaction of **4__Te** (where the H ligand bound to the N^2 is replaced by the CF_3 group) with $ONOO^-$. We calculated geometries and energies of the complex **4__Te−O(NO_2)__1**, the transition state **4__Te-TS2,** and the products **4__TeO** + NO_2^-. The calculated relative energies and important geometrical parameters of these structures are given in Table 1 and Figure 5, respectively.

As shown in Figure 5, the replacement of the H ligand bound to N^2 by CF_3 elongates the Te−N^2 bond length by 0.16 Å, and facilitates the coordination of the NO_{2-}unit to the Te-center. As a result, the calculated Te−O^2(ONO) and Te−O^3 bond lengths become shorter by 0.08 and 0.01 Å, respectively, in **4__Te−O(NO_2)__1** compared to those in **2__Te−O(NO_2)__1**. From these geometrical changes one may expect the stabilization of the Te−O^2(ONO) interaction in **4__Te−O(NO_2)__1** compared to that in **2__Te−O(NO_2)__1**. Indeed, the calculated ΔH (ΔG) of NO_2^- dissociation in **4__Te−O(NO_2)__1**, 46.6 (35.7) kcal/mol, is 10.0 (9.8) kcal/mol larger than that in **2__Te−O(NO_2)__1**, 36.6 (25.9) kcal/mol.

Similar geometrical changes in the Te−N^2 and Te−O^3 bond lengths were observed in ***n*__Te-TS2** when going from n = 2 to n = 4. The Te−N^2 bond elongated by 0.20 Å, while the Te−O^3 bond shrank by 0.02 Å. The O^--N^1 bond length was elongated by 0.10 Å, while the Te−O^2 bond shortened by 0.23 Å. As a result of these changes in geometry the barrier height at the transition state ***n*__Te-TS2** calculated from the Te−$O(NO_2)$ complex is reduced by 3.9 (3.9) kcal/mol and becomes 22.7 (23.0) kcal/mol for the complex **4__Te**.

Thus, the calculated difference Δ in the ΔH (ΔG) values of the rate-determining steps of NO_2^- dissociation and NO_3^- formation from the ***n*__Te−O(NO_2)__1** complex is −23.9 (−12.7) and −10.0 (1.0) kcal/mol for n = 4 and n = 2, respectively. These data clearly show that *the reaction of the complex* ***4__Te*** *with* $ONOO^-$ *will mainly proceed via the peroxynitrite to nitrate isomerization pathway in the gas phase. Thus, the weaker the Te−*N^2 *bond, the larger the* NO_2^-*-dissociation energy, as predicted above.*

The comparison of the data obtained for ebtellur derivative **4__Te** with those for ebselen derivative **4__Se** shows that the former significantly promotes the peroxynitrite → nitrate isomerization in the gas phase.

III.3. Role of Solvent Effects. Here, we divide our discussion into two parts. First, we discuss the solvent effects on the calculated relative energies of the reactants, intermediates, transition states, and products of the reaction **2__Te** (R = H) with PN. Second, we elucidate the roles of solvent molecules in the important steps of the reaction **4__Te** (R = CF_3) with PN, because the complex **4__Te** is predicted to catalyze the peroxynitrite → nitrate isomerization in the gas phase. In these calculations, we use water as the solvent. Note that the single-point PCM[40] calculations provide the value called ΔG (solution), which does not include zero-point energy and entropy corrections, and should be compared only with the ΔE value for the gas phase.

In Table 1, we present the calculated relative energies for the reaction ***n*__Te** + PN for n = 2 and n = 4 in water. Because the largest contributions from the solvent to the calculated

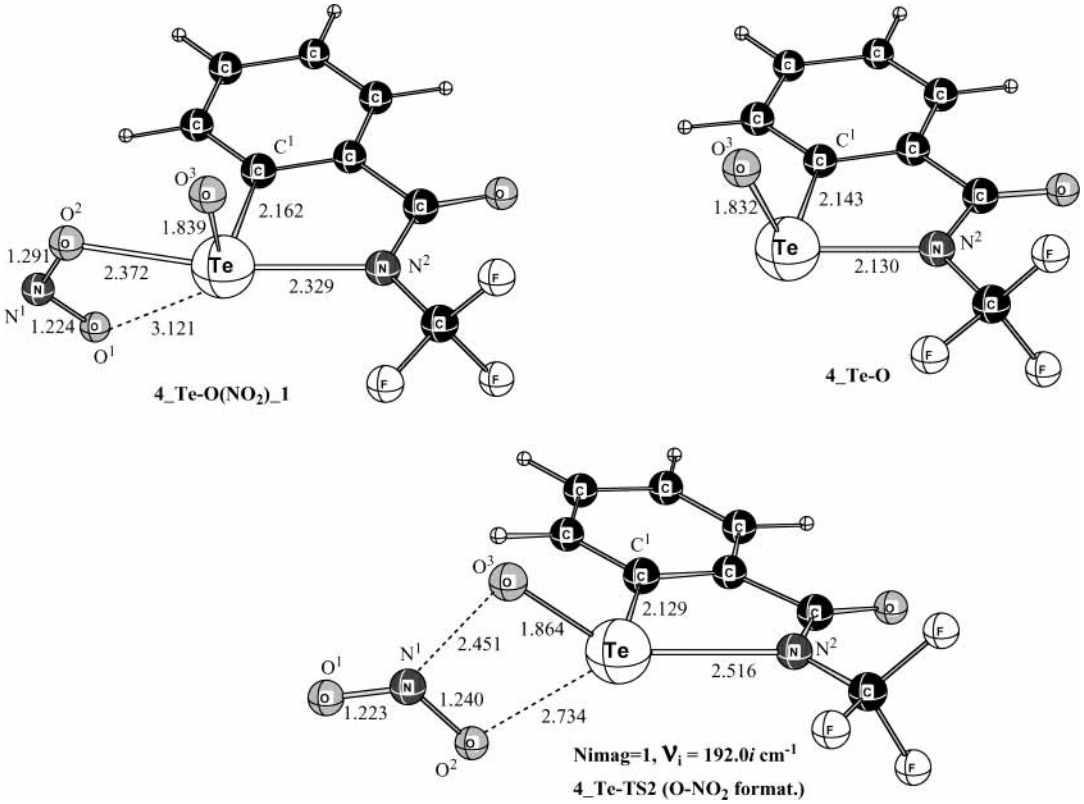

Figure 5. Calculated important geometrical parameters (distances in Å, angles in deg) of **4__Te−O−(NO₂)__1** complex, the NO_3 formation transition state, **4__Te−TS2(O−(NO₂ format)** and **4__Te−O** complex. The full geometry parameters of these species are given in the Table 1S of Supporting Information.

energetics are electrostatic terms, one may expect that solvent effects will be significant at the beginning, **2__Te** + $OONO^-$, and end, **2__TeO** + NO_2^- and **2__Te** + NO_3^-, of the reaction. Indeed, the inclusion of solvent effects dramatically (30.3, 28.8, and 19.0 kcal/mol, respectively) reduces the $ONOO^-$ complexation, and NO_2^- and NO_3^- dissociation energies: these values are calculated to be 11.0, 9.0, and −9.0 kcal/mol, respectively, in water. Meanwhile, the solvent destabilizes the O−O bond activation transition state relative to the reactants: in water the **2__Te-TS1** lies only 6.8 kcal/mol lower than the reactants, compared to 29.5 kcal/mol in the gas phase. As a result, the solvent effects reduce the calculated O−O bond cleavage barrier from 10.8 kcal/mol in the gas phase to 4.2 kcal/mol in water. However, the solvent effects only slightly increase the peroxynitrite → nitrate isomerization barrier: from 27.3 in the gas phase to 29.3 kcal/mol in water.

These data indicate that in water the reaction **2__Te** + $ONOO^-$ will occur much faster than in the gas phase and will lead to the formation of telluroxide (**2__TeO**) and NO_2^-. The peroxynitrite → nitrate isomerization will be unfavorable because the NO_3^- formation barrier (29.3 kcal/mol) is significantly higher than the NO_2^- dissociation energy (9.0 kcal/mol). It is expected that the inclusion of the entropy, temperature, and zero-point energy corrections will further enhance the NO_2^- dissociation over NO_3^- formation.

Similar solvent effects were found for the important steps of NO_2^- dissociation and NO_3^- formation in the reaction of **4__Te** with PN. The large stabilization of the NO_2^- dissociation channel by the solvent, compared to the NO_3^- formation barrier, makes the peroxynitrite → nitrate isomerization by **4__Te** impossible in water.

Previously, we have reported[26] the same trends for the reaction of ***n*__Se** with $ONOO^-$ upon including solvent effects.

IV. Conclusions

From the above discussion we may draw the following conclusions:

1. The reaction of **2__Te** with PN proceeds via **2__Te** + PN → **2__Te−PN** → **2__Te-TS1 (O−O activ)** → **2__Te−O(NO₂⁻)** pathway. The processes, NO_2^- dissociation leading to **2__Te−O** + **NO_2^-** and the NO_3^- formation via the transition state **2__Te-TS2**, starting from the complex **2__Te−O(NO_2^-)** are the rate-determining steps of the entire reaction and proceed by 36.6 (25.9) and 26.6 (26.9) kcal/mol energy loss, respectively. Since the NO_3^- formation barrier is only (1.0) kcal/mol higher than the NO_2^- dissociation energy, we predict that nitrate formation will effectively compete with the NO_2^- dissociation during the reaction of ebtellur with PN in the gas phase. Furthermore, the reaction of the ebtellur derivative with the strongest electron-withdrawing group R = CF_3, **4__Te**, with $ONOO^-$ will effectively push toward the peroxynitrite → nitrate isomerization products in the gas phase.

2. Previously[26] it was shown that the nitrate formation barrier is (7.9) kcal/mol larger than the NO_2^- dissociation barrier for the reaction of the ebselen derivative **2__Se** with PN, and, therefore, the products of the reaction **2__Se** + **PN** were predicted to be NO_2^- and selenoxide, in the gas phase. The inclusion of the strongest electron-withdrawing substituent R = CF_3 only slightly favors the peroxynitrite → nitrate isomerization pathway. The comparison of this conclusion with conclusion (1) indicates that the probability of peroxynitrite → nitrate isomerization is higher for ebtellur than ebselen derivatives in the gas phase.

3. The M−N^2 bond is extremely flexible. It changes significantly during the reaction and facilitates the reaction. It is predicted that the ebselen and ebtellur derivatives with nonexistent (or weak) M−N^2 bonds will be more active for the

PN coordination steps, the O−O bond cleavage steps, and the nitrate formation steps. Meanwhile, the ebselen and ebtellur derivatives with strong $M-N^2$ bonds are predicted to be useful for NO_2^- dissociation and selenoxide formation.

4. Solvent effects make the reaction **2__Te** + PN more facile and they stabilize the NO_2^- dissociation pathway over the nitrate formation one. They make the peroxynitrite → nitrate isomerization practically impossible, even for complex **4__Te**. The same conclusion was made[26] for the reaction of the ebselen derivatives with $ONOO^-$.

Acknowledgment is made to the Cherry L. Emerson Center of Emory University for use of its resources, which is in part supported by a National Science Foundation grant (CHE-0079627) and an IBM Shared University Research Award. This research was supported in part by a grant-in-aid for Scientific Research in Specially Promoted Research "Simulations and Dynamics for Real Systems" from the Ministry of Education, Science, Culture, and Sports of Japan.

Supporting Information Available: The Cartesian coordinates of all calculated reactants, intermediates, transition states, and products of the reaction **2__Te**+PN (Table 1S); their total energies (Table 2 S) and Mulliken charges (Table 3S); the Cartesian coordinates of all calculated important structures of the reaction of **4__Te** with PN (Table 4S), and their total energies (Table 5S); calculated ΔG (solvation) values at the PCM level for all reactants, intermediates, transition states, and products of the reaction **2__Te**+PN (Table 7S) and **4__Te**+PN (Table 8S), as well as structures of **2__Te**−**PN-*trans-trans*__1**, **2__Te**−**PN-*trans-trans*__2**, and **2 Te**−**PN-TS1(O═O activ)__*cis*** (Figure 1S). This material is available free of charge via the Internet at http://pubs.acs.org.

References and Notes

(1) See: (a) Beckman, J. S.; Beckman, T. W.; Chen, J.; Marshall, P. A.; Freeman, B. A. *Proc. Natl. Acad. Sci. U.S.A.* **1990**, *87*, 1620. (b) Beckman, J. S.; Crow, J. P. *Biochem. Soc. Transact.* **1993**, *21*, 330. (c) Ischiropoulos, H.; Zhu, L.; Beckman, J. S. *Arch. Biochem. Biophys.* **1992**, *298*, 446. (d) Huie, R. E.; Padmaja, S. *Free Radical Res. Commun.* **1993**, *18*, 195.

(2) (a) Goldstein, S.; Czapski, G.; Lind, J.; Merenyi, G. *Chem. Res. Toxicol.* **2001**, *14*, 657. (b) Edwards, J. O.; Plumb, R. C. *Prog. Inorg. Chem.* **1994**, *41*, 599. (c) Koppenol, W. H. *Met. Ions Biol. Syst.* **1999**, *36*, 597. (d) Pryor, W. A.; Squadrito, G. L. *Am. J. Physiol.* **1995**, *268*, L699 and references therein. (e) Merenyi, G.; Lind, J.; Goldstein, S.; Czapski, G. *J. Phys. Chem. A* **1999**, *103*, 5685.

(3) Kissner, R.; Koppenol, W. H. *J. Am. Chem. Soc.* **2002**, *124*, 234 and references therein.

(4) Pryor, W. A.; Gueto, R.; Jin, X.; Koppenol, W. H.; Ngu-Schwemlein, M.; Squadrito, G. L.; Uppu, P. L.; Uppu, R. M. *Free Radical Biol. Med.* **1995**, *18*, 75.

(5) (a) Beckman, J. S.; Beckman, T. W.; Chen, J.; Marshal, P. A.; Freeman, B. A. *Proc. Nat. Acad. Sci. U.S.A.* **1990**, *87*, 1620. (b) Coddington, J. W.; Hurst, J. K.; Lymar, S. V. *J. Am. Chem. Soc.* **1999**, *121*, 2438. (c) Richeson, C. E.; Mulder, P.; Bowry, V. W.; Ingold, K. U. *J. Am. Chem. Soc.* **1998**, *120*, 7211, and references therein. (d) Merenyi, G.; Lind, J.; Goldstein, S.; Czapski, G. *Chem. Res. Toxicol.* **1998**, *11*, 712.

(6) Rosen, G. M.; Freeman, B. A. *Proc. Natl. Acad. Sci. U.S.A.* **1984**, *81*, 7269.

(7) Marla, S. S.; Lee, J.; Groves, J. T. *Proc. Natl. Acad. Sci. U.S.A.* **1997**, *94*, 14243.

(8) Denicola, A.; Souza, J. M.; Radi, R. *Proc. Natl. Acad. Sci. U.S.A.* **1998**, *95*, 3566.

(9) Rachmilewitz, D.; Stamler, J. S.; Karmeli, F.; Mullins, M. E.; Singel, D. J.; Loscalzo, J.; Xavier, R. J.; Podolsky, D. K. *Gastroenterology* **1993**, *105*, 1681.

(10) Squadrito, G. L.; Jin. X.; Pryor, W. A. *Arch. Biochem. Biophys.* **1995**, *322*, 53.

(11) Lee, J.; Hunt, J. A.; Groves, J. T. *J. Am. Chem. Soc.* **1998**, *120*, 6053.

(12) Crow, J. P.; Beckman, J. S.; McCord, J. M. *Biochemistry* **1995**, *43*, 3544.

(13) Gatti, R. M.; Radi, R.; Augusto, O. *FEBS Lett.* **1994**, *348*, 287

(14) Szabo, C.; Ohshima, H. *Nitric Oxide: Biol. Chem.* **1997**,*1*, 373.

(15) (a) Halliwell, B.; Zhao, K.; Whiteman, M. *Free Radical Res.* **1999**, *31*, 651. (b) Pfeiffer, S.; Mayer, B.; Hemmens, B. *Angew. Chem., Int. Ed. Engl.* **1999**, *38*, 1715. (c) See ref 2c. (d) Groves, J. T. *Curr. Opin. Chem. Biol.* **1999**, *3*, 226. (e) Hurst, J. K.; Lymar, S. V. *Acc. Chem. Res.* **1999**, *32*, 520. (f) Trujillo, M.; Navillat, M.; Alvarez, M. N.; Peluffo, P.; Radi, R. *Analusis* **2000**, *28*, 518. (g) Radi, R.; Peluffo, P.; Alvarez, M. N.; Naviliat, M.; Cayota, A. *Free Radical Biol. Med.* **2001**, *30*, 463. (h) See ref 2d.

(16) (a) *Selenium in Biology and Human Health*; Burk, R. F., Ed.; Springer-Verlag: New York, 1994, and references therein. (b) Epp, O.; Ladenstein, R.; Wendel, A. *Eur. J. Biochem.* **1983**, *133*, 51. (c) Ren, B.; Huang, W.; Akesson, B.; Ladenstein, R. *J. Mol. Biol.* **1997**, *268*, 869.

(17) (a) Mugesh, G.; Singh, H. B. *Chem. Soc. Rev.* **2000**, *29*, 347. (b) Mugesh, G.; Panda, A.; Singh, H. B.; Punekar, N. S.; Butcher, R. J. *J. Am. Chem. Soc.* **2001**, *123*, 839. (c) Mugesh, G.; du Mont W. W.; Sies, H. *Chem. Rev.* **2001**, *101*, 2125 and references therein. (d) Briviba, K.; Roussyn, I.; Sharov, V. S.; Sies, H. *Biochem. J.* **1996**, *319*, 13.

(18) (a) Cadenas, E.; Wefers, H.; Muller, A.; Brigelius, R.; Sies, H. In *Agents and Actions Supplements*; Parnham, M. J., Winkelmann, J. Eds.; Birkhauser-Verlag: Basel, 1982; Vol. 11, p 203. (b) Parnham, M. J.; Leyck, S.; Dereu, N.; Winkelmann, J.; Graf, E. *Adv. Inflammation Res.* **1985**, *10*, 397. (c) Wendel, A.; Tiegs, G. *Biochem. Pharmacol.* **1986**, *35*, 2115. (d) Kuhl, P.; Borbe, H. O.; Fischer, H.; Romer, A.; Safayhi, H. *Prostaglandins* **1986**, *31*, 1029. (e) Parnham, M. J.; Graf, E. *Biochem. Pharmacol.* **1987**, *36*, 3095.

(19) Masumoto, H.; Kissner, R.; Koppenol, W. H.; Sies, H. *FEBS Lett.* **1996**, *398*, 179.

(20) (a) Muller, A.; Cadenas, E.; Graf, P.; Sies, H. *Biochem. Pharmacol.* **1984**, *33*, 3235. (b) Wendel, A.; Fausel, M.; Safayhi, H.; Tiegs, G.; Otter, R. *Biochem. Pharmacol.* **1984**, *33*, 3241. (c) Sies, H. *Free Radical Biol. Med.* **1993**, *14*, 313. (d) Schewe, T. *Gen. Pharmacol.* **1995**, *26*, 1153.

(21) Back, T. G.; Moussa, Z.; *J. Am. Chem. Soc.* **2002**, *124*, 12104.

(22) Jacob, C.; Arteel, G. E.; Kanda, T.; Engman, L.; Sies, H. *Chem. Res. Toxicol.* **2000**, *13*, 3 and references therein.

(23) Mugesh, G.; Panda, A.; Kumar, S.; Apte, S. D.; Singh, H. B.; Butcher, R. J. *Organometallics* **2002**, *21*, 884 and references therein.

(24) (a) Ren, X.; Xue, Y.; Liu, J.; Zhang, K.; Zheng, J.; Luo, G.; Guo, C.; Mu, Y.; Shen, J. *ChemBioChem* **2002**, *3*, 356. (b) Ren, X.; Xue, Y.; Zhang, K.; Liu, J.; Luo, G.; Zheng, J.; Mu, Y.; Shen, J. *FEBS Lett.* **2001**, *507*, 377.

(25) (a) Engman, L.; Stern, D.; Pelcman, M.; Anderson, C.-M. *J. Org. Chem.* **1994**, *59*, 1973. (b) Engman, L.; Persson, J.; Vessman, K.; Ekstorm, M.; Berglund, M.; Anderson, C.-M. *Free Radical Biol. Med.* **1995**, *19*, 441. (c) Vessman, K.; Ekstorm, M.; Berglund, M.; Anderson, C.-M.; Engman, L. *J. Org. Chem.* **1995**, *60*, 4461. (d) Anderson, C.-M.; Hallberg, A.; Brattsand, R.; Cotgreave, I. A.; Engman, L.; Persson, J. *Bioorg. Med. Chem. Lett.* **1993**, *3*, 2553. (e) Anderson, C.-M.; Brattsand, R.; Hallberg, A.; Engman, L.; Persson, J.; Moldeus, P.; Cotgreave, I. A. *Free Radical Res.* **1994**, *20*, 401. (f) Wieslander, E.; Engman, L.; Svensjo, E.; Erlansson, M.; Johansson, U.; Linden, M.; Anderson, C.-M.; Brattsand, R. *Biochem. Pharmacol.* **1998**, *55*, 573. (g) Briviba, K.; Tamler, R.; Klotz, L.-O.; Engman, L.; Cotgreave, I. A.; Sues, H. *Biochem. Pharmacol.* **1998**, *55*, 817. (i) Kanda, T.; Engman, L.; Cotgreave, I. A.; Powis, G. *J. Org. Chem.* **1999**, *64*, 8161.

(26) Musaev, D. G.; Geletii, Y. A.; Hill, G.; Hirao, K. *J. Am. Chem. Soc.* **2003**, *125*, 3877.

(27) Musaev, D. G.; Hirao, K. *J. Phys. Chem.* A **2003**, *107*, 1563.

(28) Frisch, M. J.; Trucks, G. W.; Schlegel, H. B.; Scuseria, G. E.; Robb, M. A.; Cheeseman, J. R.; Zakrzewski, V. G.; Montgomery, J. A., Jr.; Stratmann, R. E.; Burant, J. C.; Dapprich, S.; Millam, J. M.; Daniels, A. D.; Kudin, K. N.; Strain, M. C.; Farkas, O.; Tomasi, J.; Barone, V.; Cossi, M.; Cammi, R.; Mennucci, B.; Pomelli, C.; Adamo, C.; Clifford, S.; Ochterski, J.; Petersson, G. A.; Ayala, P. Y.; Cui, Q.; Morokuma, K.; Malick, D. K.; Rabuck, A. D.; Raghavachari, K.; Foresman, J. B.; Cioslowski, J.; Ortiz, J. V.; Baboul, A. G.; Stefanov, B. B.; Liu, G.; Liashenko, A.; Piskorz, P.; Komaromi, I.; Gomperts, R.; Martin, R. L.; Fox, D. J.; Keith, T.; Al-Laham, M. A.; Peng, C. Y.; Nanayakkara, A.; Gonzalez, C.; Challacombe, M.; Gill, P. M. W.; Johnson, B.; Chen, W.; Wong, M. W.; Andres, J. L.; Gonzalez, C.; Head-Gordon, M.; Replogle, E. S.; Pople, J. A. *Gaussian 98, Revision A.7*; Gaussian, Inc.: Pittsburgh, PA, 1998.

(29) (a) Becke, A. D. *Phys. Rev. A* **1988**, *38*, 3098. (b) Lee, C.; Yang, W.; Parr, R. G. *Phys. Rev. B* **1988**, *37*, 785. (c) Becke, A. D. *J. Chem. Phys.* **1993**, *98*, 5648.

(30) Dolg, M.; Wedig, U.; Soll, H.; Preuss, H. *J. Chem. Phys.* **1987**, *86*, 866.

(31) *CRC Handbook of Chemistry and Physics*, 72nd ed.; Lide, D. R., Ed.; CRC Press: Boca Raton, 1991−1992.

(32) (a) Tsai, H. H.; Hamilton, T. P.; Tsai, J. H. M.; Van der Woerd, M.; Harrison, J. G.; Jablonsky, M. J.; Beckman, J. S.; Koppenol, W. H. *J. Phys. Chem.* **1996**, *100*, 15087. (b) Tsai, J. H. M.; Harrison, J. G.; Martin,

J. C.; Hamilton, T. P.; Van der Woerd, M.; Jablonsky, M. J.; Beckman, J. S. *J. Am. Chem. Soc*. **1994**, *116*, 4115.

(33) (a) Bach, R. D.; Gluhkovtsev, M. N.; Canepa, C. *J. Am. Chem. Soc*. **1998**, *120*, 775. (b) Lynch, B. J.; Fast, P. L.; Harris, M.; Truhlar, D. G. *J. Phys. Chem.* A **2000**, *104*, 4811.

(34) See ref 26 and references therein.

(35) (a) Liang, B.; Andrews, L. *J. Am. Chem. Soc*. **2001**, *123*, 9848. (b) Bartberger, M. D.; Olson, L. P.; Houk, K. N. *Chem. Res. Toxicol.* **1998**, *11*, 710. (c) Houk, K. N.; Condroski, K. R.; Pryor, W. A. *J. Am. Chem. Soc*. **1996**, *118*, 13002. (d) Yang, D.; Tang, Y. C.; Chen, J.; Wang, X. C.; Bartberger, M. D.; Houk, K. N.; Olson, L. *J. Am. Chem. Soc*. **1999**, *122*, 11976.

(36) (a) Gonzalez, C.; Schlegel, H. B. *J. Chem. Phys.* **1989**, *90*, 2154. (b) Gonzalez, C.; Schlegel, H. B. *J. Phys. Chem.* **1990**, *94*, 5523.

(37) Wu, G.; Rovnyak, D.; Johnson, M. J. A.; Zanetti, N. C.; Musaev. D. G.; Morokuma, K.; Schrock, R. R.; Griffin, R. G.; Cummins, C. C. *J. Am. Chem. Soc*. **1996**, *118*, 10654 and references therein.

(38) Wada, M.; Nobuki, S.; Tenkyuu, Y.; Natsume, S.; Asahara, M.; Eabi, T. *J. Organomet. Chem.* **1999**, *580*, 282.

(39) Because the dissociation of **2__M−O(NO$_2$)** to NO_2^- and selenoxide is endothermic and its isomerization to **2__M-(NO$_3^-$)** requires a large energetic barrier in the gas phase, one may expect the formation of **2__M−O(NO$_2$)** as a final product.

(40) (a) Miertus, S.; Scrocco, E.; Tomasi, J. *Chem. Phys.* **1981,** *55*, 117. (b) Miertus, S.; Tomasi, J. *Chem. Phys.* **1982,** *65*, 239. (c) Cossi, M.; Barone, V.; Cammi, R.; Tomasi, J. *Chem. Phys. Lett.* **1996**, *255*, 327. (d) Cances, M. T.; Mennucci, V.; Tomasi, J. *J. Chem. Phys.* **1997**, *107*, 3032. (e) Barone, V.; Cossi, M.; Tomasi, J. *J. Comput. Chem.* **1998**, *19*, 404.